Published in final edited form as:
J Nucl Med. 2013 September ; 54(9): 1605–1612. doi:10.2967/jnumed.112.117986.

Synthesis and In Vitro/In Vivo Evaluation of Hypoxia-Enhanced ^{111}In-Bombesin Conjugates for Prostate Cancer Imaging

Zhengyuan Zhou[1], **Nilesh K. Wagh**[1], **Sunny M. Ogbomo**[1], **Wen Shi**[1], **Yinnong Jia**[1], **Susan K. Brusnahan**[1], and **Jered C. Garrison**[1,2,3,4,5]

[1]Department of Pharmaceutical Sciences, College of Pharmacy, University of Nebraska Medical Center, 985830 Nebraska Medical Center, Omaha NE, USA

[2]Center for Drug Delivery and Nanomedicine, University of Nebraska Medical Center, 985830 Nebraska Medical Center, Omaha NE, USA

[3]Department of Biochemistry and Molecular Biology, College of Medicine, University of Nebraska Medical Center, 985830 Nebraska Medical Center, Omaha NE, USA

[4]Eppley Cancer Center. University of Nebraska Medical Center, 985830 Nebraska Medical Center, Omaha NE, USA

Abstract

Receptor-targeted agents, such as BB2r-targeted peptides, have been investigated extensively in preclinical and clinical studies. In an attempt to increase the effectiveness of diagnostic and/or radiotherapeutic agents, we have begun to explore the incorporation of the hypoxia-selective prodrug 2-nitroimidazole into receptor-targeted peptides. Hypoxia is a well-known characteristic of many solid tumors, including breast, prostate and pancreatic cancers. The aim of this approach is to utilize the hypoxia trapping capability of 2-nitroimidazoles to increase the retention of the agent in hypoxic, BB2r-positive tumors. We have demonstrated that incorporation of one or more 2-nitroimidazoles into the BB2r-targeted peptide significantly increases the in vitro retention of the agent in hypoxic prostate cancer cells. The study described herein represents our first investigation of the in vivo properties of these hypoxia-enhanced BB2r-targeted agents in a PC-3 xenograft mouse model.

Method—Four ^{111}In-labeled BB2r-targeted conjugates, **^{111}In-1**, **^{111}In-2**, **^{111}In-3** and **^{111}In-4**, composed of 0–3 2-nitroimidazole moieties, respectively, were synthesized, labeled and purified. The BB2r binding affinities, externalization and protein association properties of these radioconjugates were assessed using the BB2r-positive PC-3 human prostate cancer cell line under hypoxic and normoxic environments. The in vivo biodistribution and microSPECT/CT imaging of the **^{111}In-1, ^{111}In-2 and ^{111}In-4** radioconjugates were investigated in PC-3 tumor bearing SCID mice.

[5]Corresponding Author: Phone Number: 001-402-559-3453 Fax: 001-402-559-9365 jcgarrison@unmc.edu.

No other potential conflict of interest relevant to this article was reported.

Results—All conjugates and ^{nat}In-conjugates demonstrated nanomolar binding affinities. **^{111}In-1-4** demonstrated 41.4, 60.7, 69.1 and 69.4 % retention, correspondingly, of internalized radioactivity under hypoxic conditions relative to 34.8, 35.3, 33.2 and 29.7 % retention under normoxic conditions. Protein-association studies showed significantly higher levels of association under hypoxic conditions for 2-nitroimidazole containing BB2r-targeted radioconjugates compared to control. Based on the initial 1 hour uptake in the PC-3 tumors, **^{111}In-1, ^{111}In-2** and **^{111}In-4** demonstrated tumor retentions of 1.5, 6.7 and 21.0%, respectively, by 72 h post-injection. Micro-SPECT/CT imaging studies of **^{111}In-1, ^{111}In-2** and **^{111}In-4** radioconjugates resulted in clear delineation of the tumors.

Conclusion—Based on the in vitro and in vivo studies, the BB2r-targeted agents that incorporated 2-nitroimidazole moieties demonstrated improved retention. These results indicate that further exploration into the potential of hypoxia-selective trapping agents for BB2r-targeted agents, as well as other targeted compounds, is warranted.

Keywords

tumor hypoxia; bombesin; BB2 receptor; prostate cancer; 2-nitroimidazole

According to the American Cancer Society estimates, prostate cancer is the second leading cause of death and accounts for 29% of all new cancer cases for men in the United States (1). The Gastrin-Releasing Peptide Receptor (BB2r) has been thoroughly investigated as a diagnostic and therapeutic target for prostate and other cancers due to the high expression of the receptor on neoplastic relative to normal tissues(2,3). To date, a variety of BB2r-targeted agents have been developed utilizing the BBN(7–14)NH_2 sequence (Gln-Trp-Ala-Val-Gly-His-Leu-Met-NH_2) (4–7). The developed BB2r-targeted agents, as with most low molecular weight, receptor-targeted drugs, demonstrate rapid targeting of receptor-positive tumors and swift clearance from non-targeted tissues. However, the disadvantage of many of these agents is low retention at the tumor site due to intrinsically high diffusion and efflux rates. This can substantially reduce the diagnostic and therapeutic efficacy of the agent as well as its potential for clinical translation.

Tissue hypoxia is the result of an inadequate supply of oxygen. In most solid cancers, hypoxic regions commonly exist due to a chaotic vascular architecture which impedes delivery of oxygen and other nutrients. A recent clinical investigation found that 63% (median, n = 247) of prostate tumors gave pO_2 measurements of less than 1.3 kPa (10 mm Hg, tissues less than this are generally defined as hypoxic) (8). The extent of hypoxia in tumors appears to be strongly associated with the aggressiveness of the tumor phenotype, therapeutic resistance and patient prognosis (9). Since hypoxia is not present in most normal human tissues, a variety of bioreductive, hypoxia-selective prodrugs have been developed for the purpose of diagnostic and therapeutic applications for cancer. Nitroimidazoles have been used extensively in basic and clinical investigation as diagnostic imaging agents (10,11). In hypoxic environments, nitroimidazoles undergo a series of enzymatic reductions, mediated by nitroreductase enzymes, leading to the formation of strong electrophiles which can irreversibly bind to intracellular nucleophiles thereby trapping the agent in the hypoxic tissue (12). Recently, radio halogenated nitroimidazoles, such as, [^{18}F]-fluoromisonidazole,

[^{18}F]-1-α-D-(2-deoxy-2-fluoroarabinofuranosyl)-2-nitroimidazole and [^{123}I]-iodoazomycin arabinoside have been used clinically to detect hypoxia in tumors (13–15).

One focus of our laboratory is the development of tumor-selective chemical moieties to increase the retention of receptor-targeted agents. We have begun investigating the inclusion of 2-nitroimidazoles into the structure of BB2r-targeted peptides. We have previously demonstrated that these hypoxia-enhanced BB2r-targeted peptides significantly increase retention in hypoxic PC-3 human prostate cancer cells (16). From these studies, it was determined that the proximity of the 2-nitroimidazole relative to the pharmacophore had a substantial impact on BB2r binding affinity. Herein, we present the synthesis and in vitro properties of hypoxia-enhanced BB2r-targeted radioconjugates with extended linking groups to improve BB2r binding affinity. Additionally, utilizing biodistribution and microSPECT/CT imaging studies, we report the first in vivo investigation of these agents in a PC-3 xenograft mouse model.

MATERIALS AND METHODS

Full details regarding the chemicals, equipment and methodology utilized in this manuscript are presented in the supplemental materials.

Cell lines and Xenograft Models

Prostate cancer (PC-3) cell lines were obtained from American Type Culture Collection (U.S.) and cultured under vendor recommended conditions. All animal experiments were conducted in accordance to the Principles of Animal Care outlined by National Institutes of Health and approved by the Institutional Animal Care and Use Committee of the University of Nebraska Medical Center. Four week-old Institute of Cancer Research severely combined immunodeficient (ICR SCID) mice were obtained from Charles River Laboratories (Wilmington, MA). Food and water were given ad libitum. Each animal was kept in individual cages equipped with a HEPA air filter cover in a light- and temperature-controlled environment. Bilateral PC-3 tumors were induced by subcutaneous injection of 5.0×10^6 cells in Matrigel (BD Biosciences). The tumors were allowed to grow ranging from 0.1 to 1 g (4–6 weeks post-inoculation), before the mice were utilized in pharmacokinetic studies.

Synthesis and Radiolabeling of 2-NIAA Bombesin Conjugates

Peptides 1, 2*, 3* and 4* were synthesized using an automated solid-phase peptide synthesizer (CEM) employing traditional Fmoc chemistry using a Rink Amide resin (Nova Biochem). ES-MS was used to determine the molecular mass of the prepared peptides. All conjugates were peak purified to ≥ 95% purity and quantified by RP-HPLC prior to in vitro/in vivo investigations. The 2-nitroimidazole acetic acid (2-NIAA) was synthesized as previously described (16). The 2-NIAA was manually coupled to the ε-amino group of the lysine residue for peptides **2*, 3*** and **4*** using standard amidation chemistry, peak purified by RP-HPLC and characterized by mass spectrometry. For the convenient characterization of the ^{111}In-Bombesin conjugates, naturally abundant ^{nat}In was used to substitute for ^{111}In in the ES-MS and in vitro binding studies. Isolated yields were 57.6, 28.4, 56.8 and 40.4 %

for **^{nat}In-1, ^{nat}In-2, ^{nat}In-3** and **^{nat}In-4**, respectively. All ^{nat}In-conjugates were ≥ 95% pure before mass spectrometric characterization. Radiolabeling was performed on all conjugates by mixing 100 μg samples with 37 MBq $^{111}InCl_3$ in ammonium acetate buffer (1 M, 200 μL, pH 5.5). The solution was heated for 60 min at 90 °C. The resulting specific radioactivities were 0.64, 0.71, 0.78 and 0.86 MBq/nmol for **^{111}In-1, ^{111}In-2, ^{111}In-3** and **^{111}In-4**. In order to separate radiolabeled peptides from unlabeled peptides on HPLC, 4–5 mg $CoCl_2$ were then added and incubated for 5 min at 90 °C to increase the hydrophobicity of unlabeled conjugates. The solutions were allowed to cool to room temperature and peak purified using RP-HPLC (≥95%) and concentrated using a C_{18} extraction disk. The specific activities for all peak-purified ^{111}In-conjugates are essentially the theoretical maximum of 1725 MBq/nmol. Radiolabeling yields for **^{111}In-1, ^{111}In-2, ^{111}In-3** and **^{111}In-4** were 86.3, 45.2, 71.1 and 58.8 %.

In Vitro Studies

The inhibitory concentration (IC_{50}) for all conjugates and ^{nat}In-conjugates was determined using the PC-3 human prostate cancer cell line. ^{nat}In-conjugates were used as substitutes for the corresponding ^{111}In-radioconjugates. The cell associated activity was measured using a gamma counter (LTI). Efflux studies were performed using PC-3 cells which were incubated in six-well plates (0.5×10^6/well) under hypoxic conditions (94.9% N_2, 0.1% O_2, 5% CO_2) overnight. On the day of the experiment, the medium was replaced with fresh normoxic or hypoxic medium and incubated for 2 h under normoxic (95% air, 5% CO_2) and hypoxic conditions, respectively. The cells were pre-incubated for 2 h at 37°C in the presence of 100,000 cpm of each ^{111}In-radioconjugate. At time points 0, 2, 4 and 8 h, the radioactivity of the effluxed, surface bound and internalized fractions for each radioconjugate was collected and determined using a gamma counter. For the cellular fractionation studies, the procedure for the preparation of normoxic and hypoxic PC-3 cells (2.5×10^5 / well) was carried out as outlined in the efflux studies above. At time points 2, 4 and 8 h, the cells were lysed and transferred to an Amicon Ultracel 30kDa filter with extra PBS (1mL). The samples were centrifuged at 4000×g for 10 minutes and washed with PBS (1mL×2). The radioactivity associated with the molecular weight fractions was collected and determined using a gamma counter.

Biodistribution and Small Animal SPECT/CT Imaging Studies

Biodistribution studies were carried out using PC-3 tumor bearing SCID mice. Each mouse (average weight, 20 g) received an intravenous bolus via the tail vein of 277.5 kBq (7.5 μCi) of the radio-RP-HPLC peak purified ^{111}In-radioconjugate (**^{111}In-1,^{111}In-2 or^{111}In-4**) in 100 μL of saline. The mice were sacrificed and their tissues were excised at 1, 4, 24, 48 and 72 h post injection. The excised tissues were weighed, the radioactivity measured, and the %ID or %ID/g calculated for each tissue. Blocking Studies were also investigated on ^{111}In-4 by co-injection with 300 μg of unlabeled conjugate 4 (n=3). The mice for SPECT/CT imaging studies were administered 4–11 MBq (0.108 – 0.300 mCi) of the desired BB2r-targeted peptide in 100 – 200 μL of saline via tail vein injection. At 1, 24, 48 and 72 h post injection, mice were anesthetized with 1 – 1.5 % isoflurane delivered in a 2:1 mixture of nitrous oxide/oxygen. Image acquisition was accomplished using a FLEX Triumph X-ray computed tomography/single photon emission computed tomography system (CT/SPECT)

and software (Gamma Medica, Inc., Northridge, CA) fitted with a 5-pinhole (1.0 mm/pinhole) collimator. SPECT projections (30 to 90-min acquisition time per mouse based on the amount of activity) were acquired and reconstructed using SpectReconstructionApp, followed by CT scans acquired and reconstructed using Triumph X-O 4.1.

Statistical Analysis

IC_{50} values were determined by nonlinear regression using the one-binding site model of Graphpad PRISM 5. Comparisons of each two groups for efflux studies, cellular protein analysis studies and biodistribution studies were analyzed by the 2-tailed Student t test, and P value of less than 0.05 were considered statistically significant.

RESULTS

Conjugate Synthesis and Radiolabeling

Four radioconjugates were synthesized using the DOTA-**X**-8-AOC-BBN(7–14)NH_2 paradigm (Figure 1). The yields of conjugates **1**, **2***, **3*** and **4*** ranged from 16.67 to 20.44 % as determined by RP-HPLC. The 2-NIAA coupling of conjugate **2*** and **4*** were performed by O-benzotriazole-N, N, N', N'-tetramethyl-uronium-hexafluoro-phosphate (HBTU) conjugation, whereas conjugate **3*** was coupled by using N, N'-Dicyclohexylcarbodiimide (DCC). All attempts to conjugate **3*** with 2-NIAA using HBTU resulted in poor yields (<1%). The products were purified by RP-HPLC and isolated with yields of 17.4, 26.7 and 19.0 % for conjugates **2**, **3** and **4**. RP-HPLC retention time and mass spectrometric identification of the conjugates are listed in Table 1.

In Vitro Competitive Cell-Binding Studies

The BB2r binding affinity of the conjugates and ^{nat}In-conjugates were investigated by competitive binding studies using the BB2r-positive, PC-3 cell line. All conjugates and ^{nat}In-conjugates demonstrated nanomolar binding affinities. The ^{nat}In-labeled conjugates had IC_{50} values of 7.1 ± 1.1, 7.3 ± 1.1, 5.8 ± 1.1 and 6.9 ± 1.2 nM for ^{nat}In-1-4, respectively. Slightly lower binding affinities were observed for unlabeled conjugates compared with ^{nat}In-labeled, but statistical analysis revealed no overall trend.

In Vitro Internalization and Efflux Studies

We have previously reported that the surface expression of the BB2r remains essentially unchanged under the hypoxic conditions employed in our studies (16). In these studies, **^{111}In-1,** which does not have a 2-nitroimidazole incorporated, is the control to compare the relative effectiveness of the hypoxia trapping conjugates (**^{111}In-2-4**). The PC-3 cells were first incubated in the presence of the radioconjugates for 2 h prior to the start of the efflux studies. During this incubation period, all of the radioconjugates investigated under both normoxic and hypoxic conditions demonstrated similar levels of internalization, ranging from 18 to 22% of the total radioactivity added.

The efflux of the radioconjugates over time given as a percentage of the initial internalized activity is depicted in Figure 2. Within the first 2 h of the experiment, the ^{111}In radioconjugates **1–4** under hypoxic conditions demonstrated a lower efflux rate relative to

normoxic conditions. The maximum differences of percentage effluxed radioactivity were observed at 8 h time point for **^{111}In-1-4**. Specifically, 41.4, 60.7, 69.1 and 69.4 % of initially internalized radioactivity was retained under hypoxic conditions compared with only 34.8, 35.3, 33.2 and 29.7 % retained under normoxic conditions, respectively. **^{111}In-1** also exhibited a significant decrease in clearance rate after 2 hours under hypoxic conditions. However, the increased retention showed by **^{111}In-1** is limited relative to **^{111}In-2-4** which have 2-nitroimidazoles incorporated into the structure of the radioconjugate. The radioconjugates **^{111}In-2-4** demonstrated significantly higher retention under hypoxic conditions relative to normoxic conditions ($P<0.0001$).

The internalized activity of the radioconjugate was compared as an additional means of evaluating the retention effect under normoxic and hypoxic conditions. Hypoxia enhancement factor (HEF) is defined as the ratio of the amount of activity remaining in the hypoxic cells versus the normoxic PC-3 cells of radioconjugates internalized. The HEF for each radioconjugate at each time point is depicted in Figure 3. At the initial time point, all of the radioconjugates demonstrated a similar accumulation under both normoxic and hypoxic conditions where the HEF is approximately equal to 1. At the 2 h time point, all of the radioconjugates incorporated with 2-nitroimidazole started to display significantly higher retention in hypoxic relative to normoxic cells (i.e., HEF > 1). By the 8 h time point, the **^{111}In-1-4** demonstrated an average HEF of 1.17 ± 0.12, 1.95 ± 0.28, 2.72 ± 0.35 and 3.29 ± 0.25, respectively. The radioconjugates **^{111}In-2-4** exhibited significantly higher average HEF ratios than the control. The strong positive linear relationship between the HEF and the number of 2-nitroimidazoles incorporated was confirmed by linear regression analysis ($R > 0.96$).

Cellular Protein Analysis

It is well established that 2-nitroimidazoles are reductively-activated in a hypoxic environment. This activation leads to the irreversible conjugation of the reduced 2-nitroimidazole moiety with intracellular nucleophiles (e.g., thiols), including those contained in proteins, to form adducts (17–19). In order to better elucidate the mechanism of the observed increase in retention of the 2-nitroimidazole containing BB2r-targeted agents under hypoxic conditions, the protein association properties of the conjugates were evaluated under hypoxic and normoxic environments. At the 2, 4 and 8 h post incubation time points, the PC-3 cells were lysed and centrifuged. The supernatant was then filtered using a 30 kDa centrifugal filter. The ratio of protein associated radioactivity as a percentage of total intracellular radioactivity under hypoxic conditions over the percentage of protein associated radioactivity under a normoxic environment is depicted in Figure 4. The control radioconjugates **^{111}In-1** demonstrated similar ratios, from 1.08 to 1.38, during the timespan of the experiment. The 2-nitroimidazole containing BB2r-targeted conjugates demonstrated at least one fold higher protein association under hypoxic conditions than that observed under normoxic conditions. For **^{111}In-4**, at 4 and 8 h time points, up to three fold higher hypoxic/normoxic protein association ratios were observed relative to the control. These results strongly suggest that 2-nitroimidazoles are partially responsible for this enhancement.

Biodistribution Studies

The in vivo biodistribution of the **^{111}In-1**, **^{111}In-2** and **^{111}In-4** radioconjugates were investigated in PC-3 tumor bearing SCID mice. Due to the similar efflux and protein association properties of **^{111}In-3** and **^{111}In-4,^{111}In-3** was not investigated in vivo. The results obtained from pharmacokinetic studies of **^{111}In-1**, **^{111}In-2** and **^{111}In-4** at 1, 4, 24, 48 and 72 h p.i. are summarized in Table 2. All of the investigated ^{111}In-radioconjugates demonstrated rapid blood clearance at 1 h post injection. Clearance of the radioconjugates proceeded largely through the renal/urinary system. At 1 h post injection, the highest accumulation was found in the pancreas for all three radioconjugates with 70.96 ± 15.88, 33.70 ± 27.11 and 33.04 ± 19.50 %ID/g, respectively. These results are due to the high expression of BB2r in rodent pancreas and are consistent with previous reports (5,20). The tumor retention of radioconjugate **^{111}In-4** (2.80 ± 1.18 %ID/g) at 1 h p.i. is substantially lower than **^{111}In-1** (5.82 ± 2.63%ID/g) and **^{111}In-2** (6.06 ± 3.35%ID/g). However, by the 72 h post injection time point, 1.5%, 6.7% and 21.0% of the initial 1 h uptake was retained in the tumor tissue corresponding to radioconjugates **^{111}In-1**, **^{111}In-2** and **^{111}In-4** (Figure 5). The tumor retention observed for both **^{111}In-2** (0.41 ± 0.07 %ID/g, $P<0.01$) and **^{111}In-4** (0.60 ± 0.40 %ID/g, $P<0.05$) was found to be significantly higher as compare with the control **^{111}In-1** (0.09 ± 0.10 %ID/g). With the exception of the kidneys, the addition of the 2-nitroimidazoles did not increase the non-target retention of the BB2r-targeted agents. The initial kidney uptake for all of the radioconjugates investigated was approximately 15 %ID/g at the 1 h time point. By 72 h post injection the conjugates **^{111}In-2** (2.66 ± 0.73 %ID/g) and **^{111}In-4** (8.83 ± 5.69 %ID/g) demonstrated significant retention ($P<0.05$) in the kidneys as compared to **^{111}In-1** (0.76 ± 0.67 %ID/g). In this study, the kidney retention correlated with an increase in the 2-nitroimidazole moieties of the BB2r-targeted agent. The co-injection of an excess of unlabeled conjugate **4** along with ^{111}In-4 resulted in significantly reduced radioactivity in the pancreas (1.16 ± 0.66 %ID/g), kidney (12.37 ± 7.92 %ID/g) and tumor (0.44 ± 0.34 %ID/g) at 4 h post injection ($P<0.05$, one-tailed).

Small Animal SPECT/CT Imaging Studies

Small animal SPECT/CT Imaging studies were performed in PC-3 tumor bearing SCID mice using the **^{111}In-1, ^{111}In-2,** and **^{111}In-4** radioconjugates. The whole body images and the respective axial slices of the PC-3 tumors at 1, 24, 48 and 72 h p.i. are depicted in Figure 6. At 1 h post injection, significant abdominal uptake was observed in all cases due to the accumulation of radioactivity in the G.I. tract and pancreas as previously demonstrated in the biodistribution studies. Axial slices of the PC-3 tumor for all the radioconjugates investigated exhibited substantial accumulation of radioactivity in the tumor tissue after the rapid clearance of the radioconjugates through the renal/urinary system. For **^{111}In-4** radioconjugates, conspicuous kidney retention is observed, echoing the biodistribution studies.

DISCUSSION

To determine if the incorporation of 2-nitroimidazoles would increase the retention of the radioconjugate in hypoxic PC-3 cells, we have previously synthesized four BB2r-targeted agents, that included 2-nitroimidazole moieties (16). In vitro studies showed improved

longitudinal retention of the 2-nitroimidazole containing BB2r-targeted agents in hypoxic relative to normoxic PC-3 cells. However, it was determined that the steric interference of the 2-nitroimidazole with the BB2r-targeting vector resulted in poor binding affinities which severely impeded internalization of these conjugates. In this study, an extended linker (8-AOC) was incorporated between the 2-nitroimidazole-amino acid residue and the pharmacophore. The BB2r affinities of (1–4) natural indium labeled and unlabeled conjugates versus [^{125}I-Tyr$_4$] BBN were performed for the GRP receptor using the PC-3 cell line. All ^{nat}In-BBN conjugates demonstrated nanomolar binding affinity. Based on these results, the incorporation of the 8-AOC linker has eliminated the detrimental impact of 2-NIAA side chain on pharmacophore binding.

Internalization and efflux studies demonstrated that the clearance rate of the radioconjugates containing 2-nitroimidazole was substantially lower relative to the control under hypoxic conditions. Specifically, 6.6, 25.4, 35.9 and 39.7% more retention were observed at the 8 h time point for **^{111}In-1-4** under hypoxic conditions relative to normoxic conditions. **^{111}In-3** and **^{111}In-4** which have more than one 2-nitroimidazoles (2 and 3, respectively) exhibited a higher retention effect than **^{111}In-2** which has only one 2-nitroimidazole. Inclusion of more than one hypoxia trapping moiety may increase the chances for the 2-nitroimidazole containing radioconjugates to form protein adducts thus enhancing the long-term retention of the radioconjugate in the cell. Ultimately, further investigation into the identification and quantification of the protein-adduct is needed to obtain a clearer understanding of the mechanism involved in this process. It was also interesting to note that, **^{111}In-1** exhibited a slightly lower clearance rate under hypoxic conditions, which could be due to the decreased metabolic rate under hypoxic conditions (9). With respect to the hypoxia enhancement factor, significantly higher retention in hypoxic relative to normoxic cells was observed for **^{111}In-2-4** at the 2 h time point. The HEF continued to increase for **^{111}In-1** and **^{111}In-2** throughout the experiments, but remained constant for **^{111}In-3** and **^{111}In-4** after the 4 h time point. A strong positive linear relationship between the HEF and the number of 2-nitroimidazoles incorporated was confirmed for the 8 h time points.

Cellular protein analysis of the control radioconjugate **^{111}In-1** demonstrated minimal hypoxic/normoxic cellular protein association ratios which are likely due to reversible, nonspecific binding. For the 2-nitroimidazole containing BB2r-targeted conjugates, up to a 2 fold increase was observed under hypoxic conditions. These results suggest that the significantly higher protein association ratio of 2-nitroimidazole containing radioconjugates is due, at least in part, to the irreversible binding to intracellular proteins which is consistent with the known trapping mechanism of 2-nitroimidazole.

The in vivo biodistribution of each radioconjugate was investigated in PC-3 tumor bearing SCID mice, except for **^{111}In-3** due to the similar efflux and protein association properties as **^{111}In-4**. At 1 h post injection, **^{111}In-1** and **^{111}In-2** share comparable tumor uptake, 5.82 ± 2.63 %ID/g and 6.06 ± 3.35 %ID/g, respectively. However, a substantially lower tumor uptake (2.80 ± 1.18 %ID/g) was observed for **^{111}In-4** which has three 2-nitroimidazoles incorporated. Given the similar uptake of **^{111}In-2** and **^{111}In-4** in the BB2r-positive pancreas, the reason behind the reduced tumor uptake is unclear. At 4 h post injection, most of the radioconjugates were cleared through the renal/urinary system (80 – 82 %ID) which is

consistent with other investigations of BB2r- targeted radioconjugates (20). By the 72 h post injection time point, the radioconjugates were largely cleared from most tissues, including the pancreas (21). Significant tumor retention enhancement was observed at 72 h post injection for radioconjugates **^{111}In-2** and **^{111}In-4**. Specifically, 6.7% and 21.0% of the initial 1h uptake in tumor was retained for **^{111}In-2** and **^{111}In-4,** compared with only 1.5% remaining for the control **^{111}In-1**. However, the hypoxia burden of each tumor is unknown which limits the ability to fully interpret the relationship between tumor retention effect and incorporation of the hypoxia trapping moiety. The hypoxia burden in tumor xenograft mouse models has been shown to increase (modest correlation) with an increase in tumor size, but this trend is highly dependent on the cell-line (22). Linear regression analysis of the %ID/g retention of our radioconjugates in PC-3 tumors versus tumor weight revealed no correlation between retention and tumor size. Interestingly, in the clinic, the extent of hypoxia is independent of tumor size in a variety of human cancer including head and neck, cervix and lung cancer (23–25). Further study to correlate the tumor hypoxia burden with radioconjugate retention is ongoing. Significantly lower tumor and pancreas uptake caused by co-injection of an excess of unlabeled conjugate **4** indicates that accumulation of **^{111}In-4** is largely mediated by the BB2r.

It is interesting to note the unusually high kidney retention for 2-nitroimidazole containing conjugates relative to the control conjugate. Especially for **^{111}In-4,** up to 8.83 ± 5.69 % ID/g in kidney was observed at 72 h post injection, information which has not been reported in any research related to BBN or 2-nitroimidazole based radioconjugates (5,20,26,27). Renal retention of radiolabeled targeting peptide has long been addressed as one of the dose-limiting factors in radionuclide therapy and various mechanisms have been demonstrated to be involved in high renal uptake (28). Cationic peptides are preferentially reabsorbed by the proximal tubules due to the anionic binding sites on the brush border membrane (29,30). Megalin and cubilin are known to be associated with the proximal tubular reabsorption of structurally different proteins, peptides, and drugs (31). Moreover, low or very low tissue oxygen tensions exist under physiologic conditions in kidneys, which facilitates urine concentration (32). Co-infusion of competitive inhibitors such as lysine, arginine and succinylated gelatin can reduce the reabsorption by endocytosis or transporters (33–35). In preliminary co-injection blocking studies (data not shown), both EF5 (a 2-nitroimidazole based hypoxia marker) and lysine co-injection with **^{111}In-4** can reduce the retention of radioconjugates in kidney. Further studies are needed to fully understand the mechanism of kidney retention of hypoxia trapping enhanced BBN conjugates in order to develop specific methods to reduce the renal toxicity. MicroSPET/CT images of all radioconjugates using PC-3 tumor-bearing mice at 1 h post injection (Fig. 6), showing significant abdominal uptake, are consistent with the data obtained from biodistribution studies. The PC-3 tumor xenografts in all mice are easily visualized. For the **^{111}In-4** radioconjugates, containing three 2-nitromididazoles, significant activity in kidneys was observed which strongly agrees with previously established biodistribution data.

CONCLUSION

We have synthesized three BB2r-targeted radioconjugates with 2-nitroimidazole hypoxia trapping moieties incorporated to enhance the retention in hypoxic cancer cells. In vitro

competitive binding studies indicate that inclusion of extended linker 8-AOC eliminated the detrimental effect on binding affinity that was determined in our previous report. The 2-nitroimidazole trapping moieties containing BB2r-targeted agents demonstrated significant higher retention and protein association properties in hypoxic relative to normoxic PC-3 cells. In vivo biodistribution studies revealed great potential of incorporated trapping moieties to increase the residence time of BB2r-targeted agents in PC-3 xenograft tumor. Further works are needed to clarify the mechanisms of increased retention effects at the molecular level and to correlate the tumor hypoxia burden with the retention efficacy.

Supplementary Material

Refer to Web version on PubMed Central for supplementary material.

Acknowledgments

We thank Dr. Katherine Estes for assistance in SPECT/CT imaging and the Bioimaging Core at UNMC. This study was supported by the National Cancer Institute (5 R00 CA137147) and the National Center for Research Resources (8 P20 GM103480).

REFERENCES

1. Siegel R, Naishadham D, Jemal A. Cancer statistics, 2012. CA Cancer J Clin. 2012; 62:10–29. [PubMed: 22237781]
2. Gugger M, Reubi JC. Gastrin-releasing peptide receptors in non-neoplastic and neoplastic human breast. Am J Pathol. 1999; 155:2067–2076. [PubMed: 10595936]
3. Markwalder R, Reubi JC. Gastrin-releasing peptide receptors in the human prostate: relation to neoplastic transformation. Cancer Res. 1999; 59:1152–1159. [PubMed: 10070977]
4. Abd-Elgaliel WR, Gallazzi F, Garrison JC, et al. Design, synthesis, and biological evaluation of an antagonist– bombesin analogue as targeting vector. Bioconjug Chem. 2008; 19:2040–2048. [PubMed: 18808168]
5. Garrison JC, Rold TL, Sieckman GL, et al. In vivo evaluation and small-animal PET/CT of a prostate cancer mouse model using 64Cu bombesin analogs: side-by-side comparison of the CB-TE2A and DOTA chelation systems. J Nucl Med. 2007; 48:1327–1337. [PubMed: 17631556]
6. Zhang X, Cai W, Cao F, et al. 18F-labeled bombesin analogs for targeting GRP receptor-expressing prostate cancer. J Nucl Med. 2006; 47:492–501. [PubMed: 16513619]
7. Hoffman TJ, Gali H, Smith CJ, et al. Novel series of 111In-labeled bombesin analogs as potential radiopharmaceuticals for specific targeting of gastrin-releasing peptide receptors expressed on human prostate cancer cells. J Nucl Med. 2003; 44:823–831. [PubMed: 12732685]
8. Milosevic M, Warde P, Ménard C, et al. Tumor hypoxia predicts biochemical failure following radiotherapy for clinically localized prostate cancer. Clin Cancer Res. 2012; 18:2108–2114. [PubMed: 22465832]
9. Höckel M, Vaupel P. Tumor hypoxia: definitions and current clinical, biologic, and molecular aspects. J Natl Cancer Inst. 2001; 93:266–276. [PubMed: 11181773]
10. Nunn A, Linder K, Strauss HW. Nitroimidazoles and imaging hypoxia. Eur J Nucl Med. 1995; 22:265–280. [PubMed: 7789400]
11. Krohn KA, Link JM, Mason RP. Molecular imaging of hypoxia. J Nucl Med. 2008; 49:129S–148S. [PubMed: 18523070]
12. Bolton JL, McClelland RA. Kinetics and mechanism of the decomposition in aqueous solutions of 2-(hydroxyamino) imidazoles. J Am Chem Soc. 1989; 111:8172–8181.
13. Grosu AL, Souvatzoglou M, Roper B, et al. Hypoxia imaging with FAZAPET and theoretical considerations with regard to dose painting for individualization of radiotherapy in patients with head and neck cancer. Int J Radiat Oncol Biol Phys. 2007; 69:541–551. [PubMed: 17869667]

14. Mannan RH, Somayaji VV, Lee J, Mercer JR, Chapman JD, Wiebe LI. Radioiodinated 1-(5-iodo-5-deoxy-beta-D-arabinofuranosyl)-2-nitroimidazole (iodoazomycin arabinoside: IAZA): a novel marker of tissue hypoxia. J Nucl Med. 1991; 32:1764–1770. [PubMed: 1880579]
15. Koh WJ, Rasey JS, Evans ML, et al. Imaging of hypoxia in human tumors with [F-18]fluoromisonidazole. Int J Radiat Oncol Biol Phys. 1992; 22:199–212. [PubMed: 1727119]
16. Wagh NK, Zhou Z, Ogbomo SM, Shi W, Brusnahan SK, Garrison JC. Development of hypoxia enhanced 111In-labeled Bombesin conjugates: design, synthesis, and in vitro evaluation in PC-3 human prostate cancer. Bioconjug Chem. 2012; 23:527–537. [PubMed: 22296619]
17. Brown JM, Wilson WR. Exploiting tumour hypoxia in cancer treatment. Nat Rev Cancer. 2004; 4:437–447. [PubMed: 15170446]
18. Krohn KA, Link JM, Mason RP. Molecular imaging of hypoxia. J Nucl Med. 2008; 49(Suppl 2): 129S–148S. [PubMed: 18523070]
19. Raleigh JA, Koch CJ. Importance of thiols in the reductive binding of 2-nitroimidazoles to macromolecules. Biochem Pharmacol. 1990; 40:2457–2464. [PubMed: 2176499]
20. Garrison JC, Rold TL, Sieckman GL, et al. Evaluation of the pharmacokinetic effects of various linking group using the 111In-DOTAX-BBN (7– 14) NH2 structural paradigm in a prostate cancer model. Bioconjug Chem. 2008; 19:1803–1812. [PubMed: 18712899]
21. Waser B, Eltschinger V, Linder K, Nunn A, Reubi JC. Selective in vitro targeting of GRP and NMB receptors in human tumours with the new bombesin tracer 177 Lu-AMBA. Eur J Nucl Med Mol Imaging. 2007; 34:95–100. [PubMed: 16909223]
22. Li X-F, Carlin S, Urano M, Russell J, Ling CC, O'Donoghue JA. Visualization of hypoxia in microscopic tumors by immunofluorescent microscopy. Cancer Res. 2007; 67:7646–7653. [PubMed: 17699769]
23. Nordsmark M, Bentzen SM, Overgaard J. Measurement of human tumour oxygenation status by a polarographic needle electrode: an analysis of inter-and intratumour heterogeneity. Acta Oncol. 1994; 33:383–389. [PubMed: 8018370]
24. Rasey JS, Koh W-J, Grierson JR, Grunbaum Z, Krohn KA. Radiolabeled fluoromisonidazole as an imaging agent for tumor hypoxia. Int J Radiat Oncol Biol Phys. 1989; 17:985–991. [PubMed: 2808061]
25. Fyles A, Milosevic M, Hedley D, et al. Tumor hypoxia has independent predictor impact only in patients with node-negative cervix cancer. J Clin Oncol. 2002; 20:680–687. [PubMed: 11821448]
26. Melo T, Duncan J, Ballinger JR, Rauth AM. BRU59-21, a second-generation 99mTc-labeled 2-nitroimidazole for imaging hypoxia in tumors. J Nucl Med. 2000; 41:169–176. [PubMed: 10647620]
27. Evans SM, Kachur AV, Shiue CY, et al. Noninvasive detection of tumor hypoxia using the 2-nitroimidazole [18F] EF1. J Nucl Med. 2000; 41:327–336. [PubMed: 10688119]
28. Vegt E, de Jong M, Wetzels JF, et al. Renal toxicity of radiolabeled peptides and antibody fragments: mechanisms, impact on radionuclide therapy, and strategies for prevention. J Nucl Med. 2010; 51:1049–1058. [PubMed: 20554737]
29. Behr TM, Sharkey RM, Juweid ME, et al. Reduction of the renal uptake of radiolabeled monoclonal antibody fragments by cationic amino acids and their derivatives. Cancer Res. 1995; 55:3825–3834. [PubMed: 7641200]
30. Pimm MV, Gribben SJ. Prevention of renal tubule re-absorption of radiometal (indium-111) labelled Fab fragment of a monoclonal antibody in mice by systemic administration of lysine. Eur J Nucl Med. 1994; 21:663–665. [PubMed: 7957354]
31. Christensen EI, Birn H. Megalin and cubilin: multifunctional endocytic receptors. Nat Rev Mol Cell Bio. 2002; 3:256–266. [PubMed: 11994745]
32. Brezis M, Rosen S. Hypoxia of the renal medulla—its implications for disease. New Engl J Med. 1995; 332:647–655. [PubMed: 7845430]
33. de Jong M, Rolleman EJ, Bernard BF, et al. Inhibition of renal uptake of indium-111-DTPA-octreotide in vivo. J Nucl Med. 1996; 37:1388–1392. [PubMed: 8708781]
34. Rolleman EJ, Valkema R, de Jong M, Kooij PP, Krenning EP. Safe and effective inhibition of renal uptake of radiolabelled octreotide by a combination of lysine and arginine. Eur J Nucl Med Mol Imaging. 2003; 30:9–15. [PubMed: 12483404]

35. van Eerd JE, Vegt E, Wetzels JF, et al. Gelatin-based plasma expander effectively reduces renal uptake of 111In-octreotide in mice and rats. J Nucl Med. 2006; 47:528–533. [PubMed: 16513623]

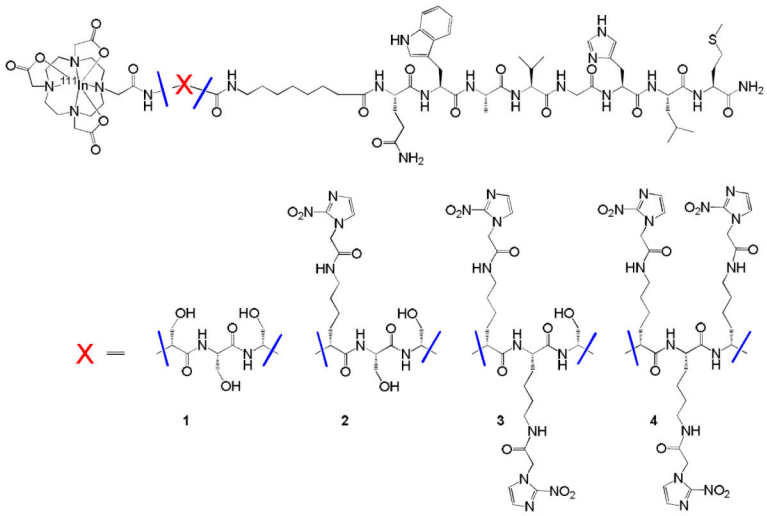

FIGURE 1.
Hypoxia enhanced ^{111}In-BB2r-targeted conjugates.

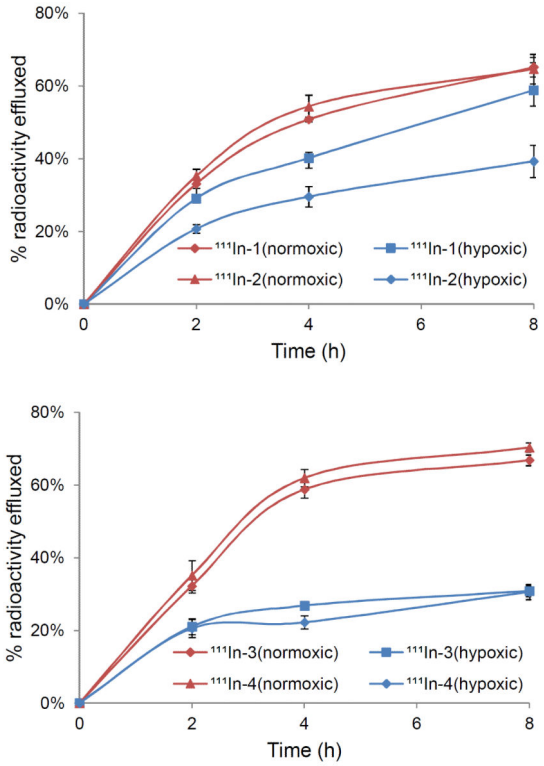

FIGURE 2.

Efflux assays depicted as percentage of initial internalized activity for the ^{111}In-radioconjugates in PC-3 cells. Values are mean ± SD (n=5).

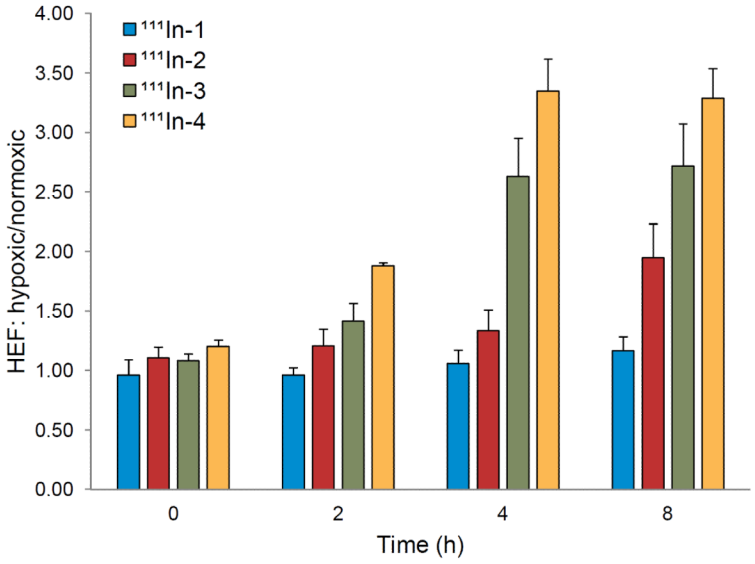

FIGURE 3.

HEF ratios for the efflux studies of ^{111}In-BB2r-targeted radioconjugates under normoxic (95% air, 5% CO_2) and hypoxic conditions (94.9% N_2, 0.1% O_2, 5% CO_2). Values are mean ± SD (n=5).

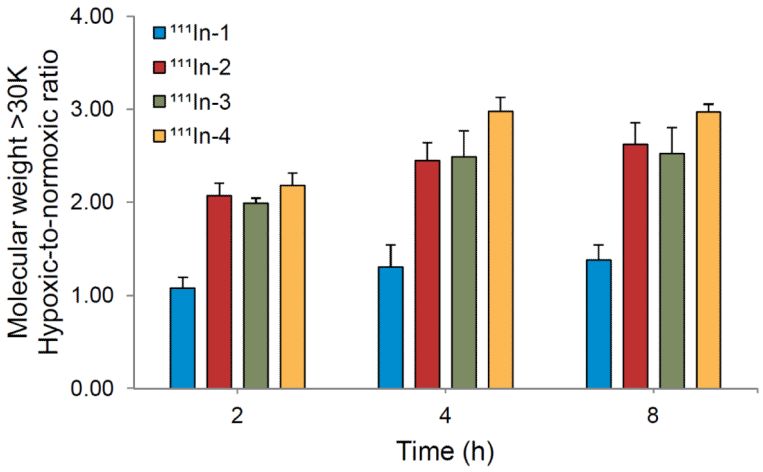

FIGURE 4.

Protein association studies under normoxic (95% air, 5% CO_2) and hypoxic (94.9% N_2, 0.1% O_2, 5% CO_2) conditions in PC-3 cells. Values are mean ± SD (n=5).

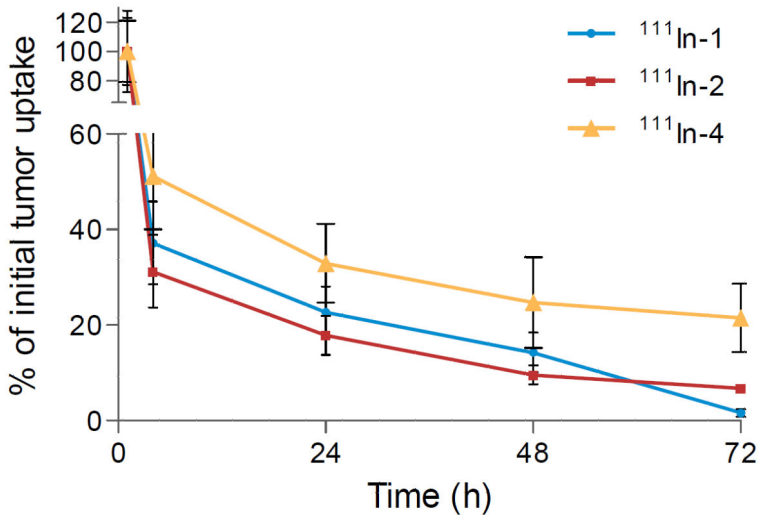

FIGURE 5.

Percentage tumor retention of ^{111}In-1, ^{111}In-2 and ^{111}In-4 in PC-3 tumor-bearing SCID mice. Values are mean ± SEM (n=4).

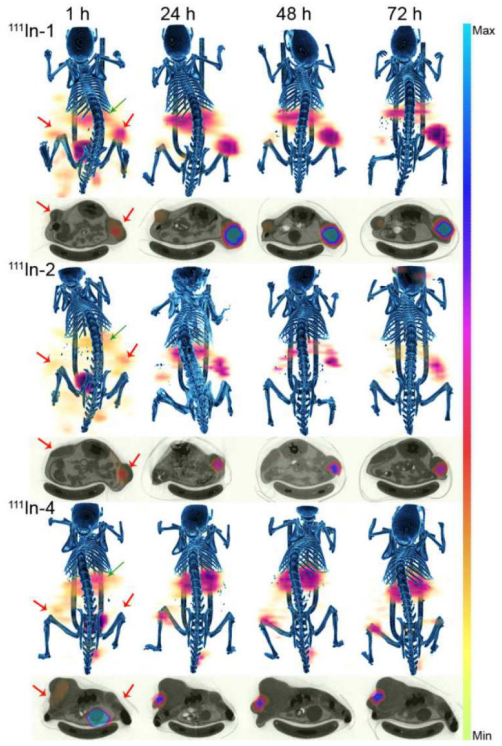

FIGURE 6.

Fused micro SPECT/CT and axial images of ^{111}In-1, ^{111}In-2 and ^{111}In-4 in PC-3 tumor-bearing mice at 1, 24, 48 and 72 h after injection. Tumors and kidneys are indicated by red and green arrows respectively.

TABLE 1

Mass spectrometric and RP-HPLC characterization of conjugates

	Analogue	Molecular Formula	MS Calculated	MS Observed	RP-HPLC Retention Time[b]/min	IC_{50}[b]/nM
1	DOTA-(D)S-(D)S-(D)S-8 AOC–BBN(7-14) NH_2	$C_{76}H_{121}N_{21}O_{23}S$	1728.9	1729.6	12.08	11.3 ± 1.4
2*	DOTA-(D)K-(D)S-(D)S-8 AOC–BBN(7-14) NH_2	$C_{79}H_{128}N_{22}O_{22}S$	1770.1	1770.8	7.73	-
3*	DOTA-(D)K-(D)K-(D)S-8 AOC–BBN(7-14) NH_2	$C_{82}H_{135}N_{23}O_{21}S$	1811.1	1812.1	12.37	-
4*	DOTA-(D)K-(D)K-(D)K-8 AOC–BBN(7-14) NH_2	$C_{85}H_{142}N_{24}O_{20}S$	1852.2	1852.5	9.32	-
2	DOTA [(D)K (2-NIAA)--(D)S-(D)S-8 AOC]–BBN(7-14) NH_2	$C_{84}H_{131}N_{25}O_{25}S$	1923.1	1923.9	14.5	12.6 ±1.4
3	DOTA [(D)K (2-NIAA)- (D)K (2-NIAA)-(D)S-8 AOC-BBN(7-14) NH_2	$C_{92}H_{141}N_{29}O_{27}S$	2117.3	2118.1	8.48	17.1 ± 1.2
4	DOTA [(D)K (2-NIAA)- (D)K (2-NIAA)-(D)K (2-NIAA)-8 AOC] –BBN(7-14) NH_2	$C_{100}H_{151}N_{33}O_{29}S$	2311.5	2312.0	9.87	20.1 ±1.3
ln-1	ln-DOTA-(D)S-(D)S-(D)S-8 AOC–BBN(7-14) NH_2	$C_{76}H_{118}{}^{114}lnN_{21}O_{23}S$	1839.7	1840.2[a]	5.60	7.1 ± 1.1
ln-2	In-DOTA [(D)K (2-NIAA)–(D)S-(D)S-8 AOC]–BBN(7-14) NH_2	$C_{84}H_{128}{}^{114}lnN_{25}O_{25}S$	2034.9	2035.0[a]	7.87	7.3 ± 1.1
ln-3	In-DOTA [(D)K (2-NIAA)-(D)K (2-NIAA)-(D)S-8 AOC-BBN(7-14) NH_2	$C_{92}H_{138}{}^{114}lnN_{29}O_{27}S$	2229.1	2229.5[a]	9.2	5.8 ± 1.1
ln-4	In-DOTA [(D)K (2-NIAA)- (D)K (2-NIAA)-(D)K (2-NIAA)-8 AOC] –BBN(7-14) NH_2	$C_{100}H^{148}lnN_{33}O_{29}S$	2423.3	2423.1[a]	10.55	6.9 ± 1.2

[a] For convenient mass spectra analysis ^{111}ln was replaced by ^{nat}ln.

[b] RP-HPLC methods described in supplemental materials.

Values represent mean ± SEM (n=6)

TABLE 2

Biodistribution Studies in PC-3 Tumor-Bearing SCID mice[a]

Tissue (%ID/g)	1 h p.i.	4 h p.i.	24 h p.i.	48 h p.i.	72 h p.i.
			^{111} In-I		
blood	0.11 ± 0.22	0.00 ± 0.00	0.00 ± 0.00	0.00 ± 0.00	0.00 ± 0.00
heart	0.00 ± 0.00	0.00 ± 0.00	0.00 ± 0.00	0.00 ± 0.00	0.00 ± 0.00
lung	0.21 ± 0.40	0.02 ± 0.03	0.00 ± 0.00	0.00 ± 0.00	0.00 ± 0.00
liver	0.40 ± 0.32	0.09 ± 0.11	0.03 ± 0.03	0.00 ± 0.00	0.00 ± 0.00
pancreas	70.96 ± 15.88	37.17 ± 10.52	12.07 ± 3.05	6.51 ± 2.26	0.00 ± 0.00
stomach	5.87 ± 3.63	1.02 ± 0.72	0.34 ± 0.26	0.11 ± 0.23	0.00 ± 0.00
small intestine (%ID)	8.15 ± 2.93	2.04 ± 0.59	0.96 ± 0.52	0.66 ± 0.18	0.02 ± 0.04
large intestine (%ID)	5.07 ± 1.26	4.74 ± 2.08	1.62 ± 0.54	1.71 ± 0.87	0.46 ± 0.28
kidney	13.41 ± 5.84	4.82 ± 1.60	2.18 ± 0.67	1.38 ± 1.01	0.76 ± 0.67
tumor	5.82 ± 2.63	2.16 ± 1.01	1.32 ± 0.62	0.83 ± 0.48	0.09 ± 0.10
muscle	0.00 ± 0.00	0.00 ± 0.00	0.00 ± 0.00	0.00 ± 0.00	0.00 ± 0.00
bone	0.00 ± 0.00	0.00 ± 0.00	0.00 ± 0.00	0.00 ± 0.00	0.00 ± 0.00
brain	0.00 ± 0.00	0.00 ± 0.00	0.00 ± 0.00	0.00 ± 0.00	0.00 ± 0.00
excretion[b] (%ID)	35.88 ± 14.38	82.06 ± 4.65	91.07 ± 1.75	93.42 ± 3.26	98.44 ± 0.48
			^{111} In-2		
blood	1.21 ± 0.61	0.00 ± 0.00	0.02 ± 0.02	0.00 ± 0.00	0.00 ± 0.00
heart	0.00 ± 0.00	0.00 ± 0.00	0.00 ± 0.00	0.00 ± 0.00	0.00 ± 0.00
lung	1.21 ± 0.98	0.00 ± 0.00	0.00 ± 0.00	0.00 ± 0.00	0.00 ± 0.00
liver	0.87 ± 0.38	0.15 ± 0.05	0.13 ± 0.05	0.08 ± 0.01	0.06 ± 0.02
pancreas	33.70 ± 27.11	14.01 ± 13.97	1.98 ± 1.35	0.25 ± 0.17	0.22 ± 0.12
stomach	1.51 ± 1.69	0.49 ± 0.20	0.06 ± 0.08	0.07 ± 0.09	0.04 ± 0.08
small intestine (%ID)	4.62 ± 1.42	1.44 ± 0.61	0.23 ± 0.10	0.12 ± 0.06	0.02 ± 0.02
large intestine (%ID)	2.02 ± 0.7	3.82 ± 1.11	0.57 ± 0.18	0.35 ± 0.14	0.15 ± 0.04
kidney	14.88 ± 4.55	5.09 ± 1.70	3.74 ± 1.65	2.03 ± 0.42	2.66 ± 0.73
tumor	6.06 ± 3.35	1.89 ± 0.92	1.08 ± 0.49	0.58 ± 0.24	0.41 ± 0.07
muscle	1.69 ± 1.72	0.12 ± 0.25	0.00 ± 0.00	0.00 ± 0.00	0.00 ± 0.00
bone	0.71 ± 0.42	0.14 ± 0.15	0.00 ± 0.00	0.00 ± 0.00	0.00 ± 0.00
brain	0.02 ± 0.05	0.00 ± 0.00	0.00 ± 0.00	0.00 ± 0.00	0.00 ± 0.00
excretion[b] (%ID)	17.26 ± 15.53	81.24 ± 8.28	94.89 ± 0.67	96.10 ± 0.61	95.90 ± 0.95
			^{111} In-4		
blood	0.75 ± 0.54	0.00 ± 0.00	0.00 ± 0.00	0.00 ± 0.00	0.00 ± 0.00
heart	0.73 ± 1.46	0.00 ± 0.00	0.00 ± 0.00	0.00 ± 0.00	0.00 ± 0.00
lung	0.61 ± 1.04	0.41 ± 0.82	0.00 ± 0.00	0.00 ± 0.00	0.00 ± 0.00
liver	0.38 ± 0.36	0.30 ± 0.24	0.20 ± 0.45	0.45 ± 0.33	0.01 ± 0.02
pancreas	33.04 ± 19.50	7.73 ± 2.70	0.62 ± 1.25	0.06 ± 0.12	0.00 ± 0.00
stomach	0.50 ± 0.75	0.00 ± 0.00	0.00 ± 0.00	0.00 ± 0.00	0.00 ± 0.00
small intestine (%ID)	3.18 ± 1.77	1.00 ± 0.59	0.25 ± 0.18	0.01 ± 0.01	0.09 ± 0.14

Tissue (%ID/g)	1 h p.i.	4 h p.i.	24 h p.i.	48 h p.i.	72 h p.i.
large intestine (%ID)	2.16 ± 0.94	2.38 ± 1.05	0.83 ± 0.16	0.57 ± 0.33	0.24 ± 0.27
kidney	17.90 ± 10.88	25.79 ± 4.66	23.40 ± 12.33	12.87 ± 2.76	8.83 ± 5.69
tumor	2.80 ± 1.18	1.43 ± 0.62	0.92 ± 0.46	0.69 ± 0.53	0.60 ± 0.40
muscle	0.00 ± 0.00	0.00 ± 0.00	0.00 ± 0.00	0.00 ± 0.00	0.00 ± 0.00
bone	0.00 ± 0.00	0.00 ± 0.00	0.00 ± 0.00	0.00 ± 0.00	0.00 ± 0.00
brain	0.00 ± 0.00	0.00 ± 0.00	0.00 ± 0.00	0.00 ± 0.00	0.00 ± 0.00
excretion[b] **(%ID)**	61.95 ± 23.27	80.86 ± 2.63	87.21 ± 2.75	91.55 ± 1.73	93.85 ± 2.78

[a]Organ uptake values expressed as %ID/g and values are mean ± SD (n=4) unless otherwise noted.

[b]Excretion values were calculated using the activity values associated with the excreted urine, bladder, and fecal material contents at the time of sacrifice.